2010

Three-dimensional simulations of the orientation and structure of reconnection X-lines

R. Schreier

M. Swisdak

J. F. Drake

P. A. Cassak

Three-dimensional simulations of the orientation and structure of reconnection X-lines

R. Schreier,[1] M. Swisdak,[1, a)] J. F. Drake,[1] and P. A. Cassak[2]

[1)] *IREAP, University of Maryland, College Park, MD 20742-3511, USA*

[2)] *Department of Physics, West Virginia University, Morgantown, West Virginia 26506, USA*

(Dated: 27 April 2018)

This work employs Hall magnetohydrodynamic (MHD) simulations to study the X-lines formed during the reconnection of magnetic fields with differing strengths and orientations embedded in plasmas of differing densities. Although random initial perturbations trigger the growth of X-lines with many orientations, at late time a few robust X-lines sharing an orientation reasonably consistent with the direction that maximizes the outflow speed, as predicted by Swisdak and Drake [Geophys. Res. Lett., **34**, L11106, (2007)], dominate the system. The existence of reconnection in the geometry examined here contradicts the suggestion of Sonnerup [J. Geophys. Res. **79**, 1546 (1974)] that reconnection occurs in a plane normal to the equilibrium current. At late time the growth of the X-lines stagnates, leaving them shorter than the simulation domain.

PACS numbers: 52.35.Vd, 94.30.cp, 96.60.lv, 52.65.Kj

[a)] Electronic mail: swisdak@umd.edu

According to the frozen-in theorem of MHD, two adjoining collisionless plasmas with different densities, temperatures, and magnetic fields cannot alter their magnetic topology, and hence transport across their common boundary is prohibited. Magnetic reconnection violates this constraint as, for example, when solar wind plasma penetrates the Earth's magnetosphere or fusion plasma escapes from a tokamak core during a disruption. The questions of whether and how reconnection takes place for arbitrary plasma conditions are important for these and other systems.

Consider two plasmas threaded by magnetic fields $\mathbf{B}_1$ and $\mathbf{B}_2$ of arbitrary relative orientation and separated by a planar surface, the $x-z$ plane in Fig. 1. We define the y axis to be perpendicular to the discontinuity plane, the z axis to parallel the X-line, and the x axis to complete the right-handed triplet. Let θ be the shear angle between the two fields and α be the unknown angle between $\mathbf{B}_1$ and the X-line. In the highly symmetric cases often considered in theory and simulations α can frequently be easily deduced (e.g., $\alpha = 90°$ for $\mathbf{B_1} = -\mathbf{B_2}$,). For more general configurations, however, no obvious choice exists, nor is it even clear that a single X-line orientation will dominate the system. Sonnerup[1] argued that α is determined by requiring that the currents in the reconnection plane vanish or, equivalently, that the components of the fields parallel to the X-line (the guide fields) be equal. As a consequence, no reconnection occurs in this scenario when $\cos\theta \geq B_1/B_2$ (assuming, as in Fig. 1, $B_1 \leq B_2$), since no component of the field changes sign across the discontinuity.

Others[2,3] have questioned this choice on both theoretical and observational grounds. For example, although the Sonnerup criterion implies that reconnection between plasmas with small shear angles occurs infrequently, in situ observations in the solar wind suggest the contrary to be true[4–7]. In fact, most reconnection events in the solar wind occur at shear angles $< 90°$[5,7].

As an alternative, Swisdak and Drake[8] proposed that the X-line orients itself so as to maximize the speed of the Alfvénic outflow. The outflow speed for plasmas with reconnecting components B_{1x} and B_{2x} and mass densities ρ_1 and ρ_2 is[8,9]

$$v_{\mathrm{out}}^2 = \frac{B_{1x} + B_{2x}}{4\pi}\left(\frac{\rho_1}{B_{1x}} + \frac{\rho_2}{B_{2x}}\right)^{-1}. \tag{1}$$

Writing this expression in terms of α and maximizing with respect to α for a fixed θ determines the X-line orientation. Since v_{out} always has a local maximum between $\alpha = 0$ and $\alpha = \theta$ reconnection occurs for any $\theta \neq 0$. An alternative suggestion holds that maximiz-

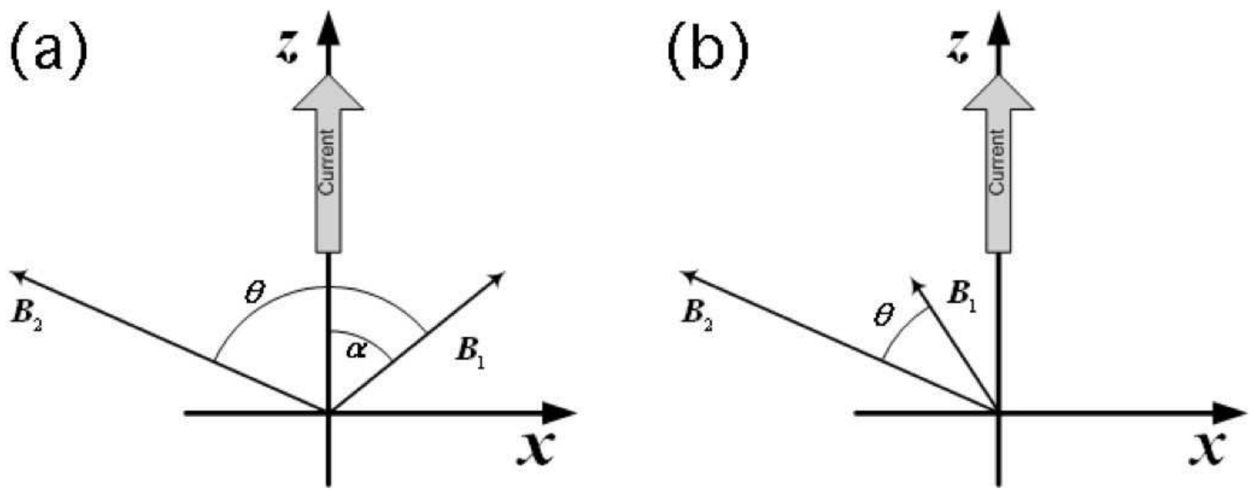

FIG. 1. Field line geometries related to the Sonnerup[1] hypothesis. The reconnecting plasmas with fields B_1 and B_2 occupy the spaces $y > 0$ and $y < 0$. In both panels the X-line parallels $\hat{z}$, reconnection occurs in the $x - y$ plane, and the fields are oriented such that the components parallel to the X-line are equal. Sonnerup[1] proposed that reconnection occurs when the x-components of B_1 and B_2 are anti-parallel (a), and that it otherwise does not (b).

ing a related quantity, the normalized reconnection rate, determines the X-line orientation (M. A. Shay, private communication).

In this work we perform 2-D and 3-D two-fluid simulations of reconnection between asymmetric plasmas in order to explore the generic development of X-lines. We first use a 2-D simulation to demonstrate magnetic reconnection in a system with small shear angle with the caveat that, since 2-D simulations artificially impose the orientation of the X-line, studying the full development of the system necessitates a 3-D domain. Hence, we also consider a 3-D simulation of the same system. In previous investigations of 3D Hall reconnection[10–12], the initial configuration of anti-parallel fields confined nascent X-lines to one plane between the two plasmas. Initially localized X-lines grew in the direction of the electron current and, in some cases, extended over almost the entire computational domain. For the more general situation considered here, X-lines in the linear stage of development grow on different planes, known as rational surfaces, and undergo more complex interactions. We find that X-lines of several different orientations are excited at early times, but eventually only a few modes dominate. Interestingly, and in contrast to previous investigations[10,11], the X-lines' length stagnates at a finite value that is shorter than the simulation domain.

For our initial equilibrium we employ a double tearing mode configuration with magnetic field components

$$B_x(y) = \tanh\left(\frac{y + L_y/4}{w_0}\right) - \tanh\left(\frac{y - L_y/4}{w_0}\right) - 1 \tag{2}$$

and

$$B_z(y) = -\frac{1}{\sqrt{2}}\tanh\left(\frac{y + L_y/4}{w_0}\right) + \frac{1}{\sqrt{2}}\tanh\left(\frac{y - L_y/4}{w_0}\right) + 2\sqrt{2}, \tag{3}$$

where $w_0 = 0.5$ is the initial width of the current sheet (the normalization is described later). The asymptotic fields have components $(B_x, B_y, B_z) = (1, 0, \sqrt{2})$ and $(-1, 0, 2\sqrt{2})$. Total pressure is balanced using a non-uniform number density n given by

$$n = \frac{1}{T}\left(P_a - \frac{B^2}{2}\right), \tag{4}$$

where the temperature $T = 1.0$ is uniform, B is the magnitude of the magnetic field, $P_a = 5.5$ is a constant, and the factor of 2 in the denominator arises from our code's normalization. For this configuration $\rho_1 = 4$, $\rho_2 = 1$, $B_1 = \sqrt{3}$, $B_2 = 3$, and the shear angle $\theta = 54.7°$. This system represents the limiting case described by Sonnerup[1] since $\cos\theta = B_1/B_2$.

The numerical simulations use the Hall-MHD code F3D[13]. It explicitly advances the dynamical variables (magnetic field, mass density, and ion velocity) with the second-order trapezoidal leapfrog method[14] in time and fourth-order finite differencing in space. Periodic boundary conditions are applied in all directions. Variables are measured in normalized units: lengths to the ion inertial length $d_i = (m_i c^2/4\pi n_0 e^2)^{1/2}$, velocities to the Alfvén speed $c_A = B_0/(4\pi m_i n_0)^{1/2}$, densities to an arbitrary value n_0, pressures to $P_0 = m_i n_0 c_A^2$, magnetic fields to an arbitrary field strength B_0, temperatures to $m_i c_A^2$ and electric fields to $E_0 = c_A B_0/c$. Here c is the speed of light, and m_i and e are the mass and charge of the ions, respectively.

The grid cells have a length of 0.2 on each side. No explicit viscosity or resistivity are applied, but a fourth-order diffusion coefficient of 10^{-3} damps noise at the grid scale. The electron-to-ion mass ratio is $m_e/m_i = 1/25$. Since the electron inertial length $d_e = d_i\sqrt{m_e/m_i}$ equals the cell size, the simulations do not describe the details of the electron dynamics.

To determine whether reconnection can occur between the fields of Eqs. (2) and (3), we first perform a 2-D simulation. The computational domain has size $L_x \times L_y = 51.2 \times 25.6$ and no variations are allowed in the z direction (i.e., $\partial/\partial z = 0$). We initiate reconnection

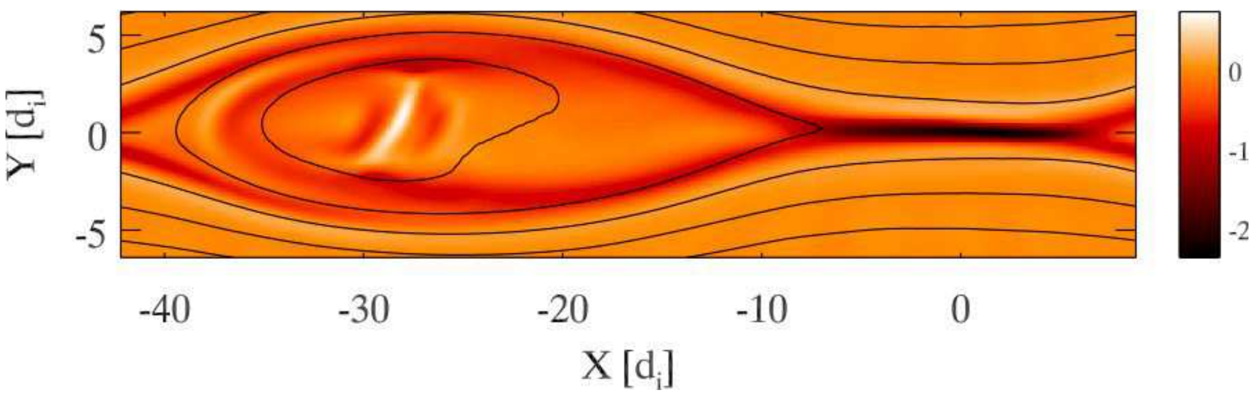

FIG. 2. (Color online) Out-of-plane current density J_z for the lower sheet in the 2-D simulation at $t = 156$ with over-plotted magnetic field lines. The other sheet exhibits similar behavior.

with random magnetic perturbations of amplitude $10^{-3}B_0$. The perturbations are generated in k-space with maximum wavenumbers of $k_x = k_y = 15$. Setting the initial perturbation amplitude 100 times smaller produces similar final results.

During the early stages of the simulation, strong out-of-plane currents develop, indicating the existence of magnetic reconnection. As the system evolves, multiple X-lines form, move along the x-axis, and merge, eventually leaving just one reconnection site. The out-of-plane current density of the lower current sheet after this merging is shown in Fig. 2. Following some initial fluctuations, caused by the interactions of multiple X-lines, the normalized reconnection rate stabilizes at a relatively steady value of ~ 0.02.

This simulation demonstrates that reconnection can occur in a plane that includes equilibrium currents in a geometry where the model of Sonnerup[1] suggests it should not. However, since the geometry of the computational domain determines the X-line orientation it did not establish whether an optimal orientation exists. Doing that requires a full 3D system, in which X-lines are free to develop in any direction. Our 3D simulation uses the same initial equilibrium as the 2D run, but applied on a computational domain of size $L_x \times L_y \times L_z = 51.2 \times 51.2 \times 409.6$, and a grid scale in the out-of-plane direction of 0.2. Initial perturbations on the magnetic field in the z direction have a maximum wavenumber of $k_z = 5$.

In the linear theory of the tearing mode in periodic systems, reconnection can only occur at discrete locations, called rational surfaces, where $\mathbf{k} \cdot \mathbf{B}_0 = 0$ ($\mathbf{k}$ is the wavenumber of the linear mode and $\mathbf{B}_0$ is the equilibrium field). Due to the periodicity of the domain, the wavenumbers of the linear instability must take the form $k_x = 2\pi m/L_x$ and $k_z = 2\pi n/L_z$, where m and n are integers. This establishes rational surfaces at the locations satisfying

$$\frac{B_x(y)}{B_z(y)} = -\frac{nL_x}{mL_z}. \tag{5}$$

Since $L_z/L_x = 8$ several linear modes with $n \neq 0$ can grow in the current layer. Once they exit the linear regime interactions between different modes allow them to no longer respect the rational surfaces

To reiterate, the model of Sonnerup[1] predicts that reconnection will not occur in this system. In contrast, Swisdak and Drake[8] predict that reconnection will occur with the X-line at an angle α given by the root of the equation

$$\begin{aligned} 0 = \quad & \frac{\rho_2}{\rho_1}\sin^2\alpha\left[\sin(\theta-2\alpha) - \frac{B_2}{B_1}\sin(2\theta-2\alpha)\right] \\ & + \frac{B_2}{B_1}\sin^2(\theta-\alpha)\left[\sin 2\alpha + \frac{B_2}{B_1}\sin(\theta-2\alpha)\right] \end{aligned} \tag{6}$$

lying between 0 and θ. Numerically solving for the parameters of the present system — $B_2/B_1 = \sqrt{3}, \rho_2/\rho_1 = 1/4$, and $\theta = 54.7^\circ$ — yields $\alpha = 34.3^\circ$.

The early evolution of the 3-D simulation mirrors that of the 2-D run, in that both current sheets develop multiple X-lines separated by bulges in which reconnected flux accumulates. In Fig. 3 we present cuts at $t = 84$ (relatively early in the simulation) of J_z in the x-y plane for four values of z separated by $L_z/4$. For the 2-D simulation of Fig. 2 the X-lines necessarily parallel the z-axis, but that is not the case in Fig. 3.

While in the 2D case topological constraints make the identification of X-lines straightforward, in three dimensions the situation is more complicated, particularly when, as is the case here, no 3-D nulls exist in the system[15]. In this work we take an empirical approach to identifying reconnection sites by examining isosurfaces of the current density $J_{xz} = \sqrt{J_x^2 + J_z^2}$. (We use J_{xz} in order to avoid favoring a particular X-line orientation in the $x - z$ plane, although in practice we find that $J_z \gg J_x$.) Fig. 4 shows two values of the isosurface level at two different times. The regions of strong current, which map the X-lines, form extended structures in the x-z plane at various angles with respect to the z axis. At $t = 84$ (panels (a) and (b)) multiple X-lines are present, but by $t = 201$ (panels (c) and (d)) only a few distinct orientations dominate the system. Although the predominant X-line orientation at $t = 201$ is horizontal, there are some interesting features that appear to be aligned with the asymptotic magnetic fields. Although many of the weaker examples (for instance, the thin

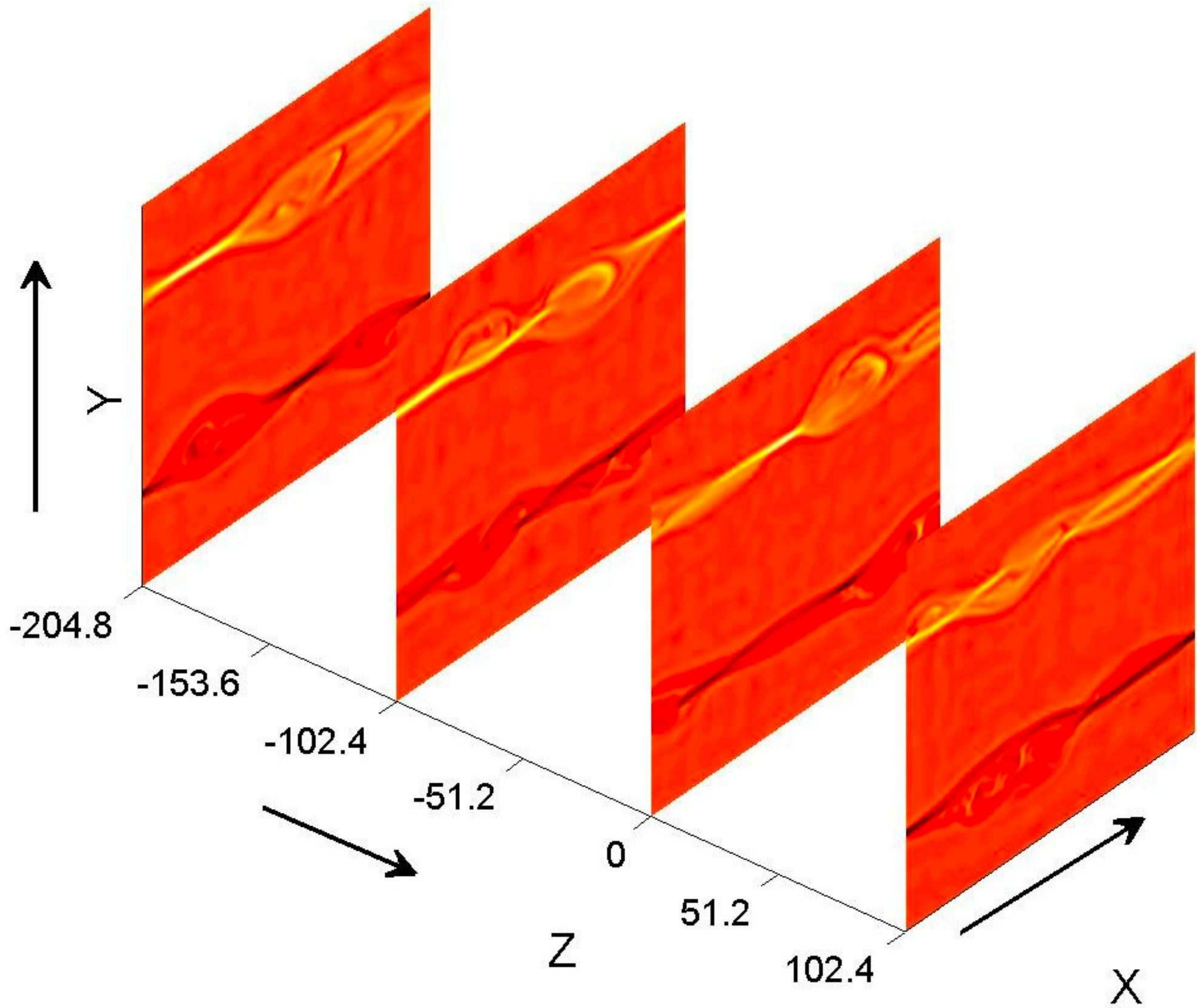

FIG. 3. (Color online) Slices of J_z in the $x - y$ plane of the 3-D domain at $t = 84$. The upper (lower) current sheet is described by bright (dark) colors, representing positive (negative) currents.

structures at $z \approx 40$ and $x \approx 20$ in panel (c)) are field-aligned currents not directly associated with reconnection, the strongest instances (e.g., the structure at $-170 \leq z \leq -120$ and $-10 \leq x \leq 10$ in panel (d)) correspond to X-lines. Reconnection of the initial asymptotic fields cannot be occurring at such sites and, in fact, cuts through these features (not shown) reveal that the local reconnecting fields differ significantly from the initial asymptotic values.

To evaluate the orientation of the X-lines quantitatively, we project the isosurfaces on the $x - z$ plane and detect the edges with the Canny method[16], a standard image processing tool that finds edges by looking for local maxima of the gradient. The gradient is calculated using the derivative of a Gaussian filter. The method uses two thresholds to detect strong and weak edges and includes the weak edges in the output only if they are connected to strong edges. In Fig. 5, the edges of the isosurface projection of Fig. 4d are shown in black. Due to imperfections in either the image data or the edge detector, there may be missing points on the desired curve.

The grouping of the extracted edge features to determine the X-line orientation is done with the Hough transform[17]. For each image pixel and its neighborhood, the Hough transform algorithm determines whether an edge exists at that pixel. The pixels lying along the highest values of parametric lines represent potential lines in the input image. Small gaps are automatically filled, and the lines are identified while a threshold is applied so that only lines longer than that value are considered. The red lines in Fig. 5 are the identified lines of the Hough transform, and clearly map the X-line. By simply averaging the various orientations identified in Fig. 5, we find that at $t = 201$ the X-line is oriented at an angle of $\phi \approx 0.6 \pm 8.5°$ with respect to the z-axis, which corresponds to $\alpha_{\rm sim} = \arctan(1/\sqrt{2}) + \phi \approx 35.9° \pm 8.5°$.

We have demonstrated that magnetic reconnection can occur between magnetic fields of small shear angle, in particular in configurations in which there is no anti-parallel component of the magnetic field in the plane perpendicular to the equilibrium current. This result disagrees with the model of Sonnerup[1]. In the initial stages of the simulation, we see the growth of X-lines with multiple orientations. By late time, however, one direction predominates. The orientation of this X-line, $\alpha_{\rm sim} = 35.9° \pm 8.5°$, agrees with the prediction of Swisdak and Drake[8], $\alpha_{SD} = 34.3°$. The existence of many short X-lines with differing orientations early in the simulation demonstrates that L_z does not play a limiting role and hence that the size of the computational domain probably does not affect our results.

The value of α_{SD} predicted by Swisdak and Drake[8] is the angle that maximizes the outflow speed from the X-line when the reconnecting fields have their asymptotic initial values. The strong diagonal features in Fig. 4d discussed above, on the other hand, are due to the reconnection of significantly perturbed fields. (The density contrast, ρ_2/ρ_1, remains essentially constant.) Applying the criterion of Eq. 6 to the perturbed fields yields orientations roughly consistent with those observed in the simulation. It is unclear, however, if there is some overarching reason why the local reconnecting fields would be reconfigured in such a way as to generate X-lines that parallel the original asymptotic fields, or if the alignment in this case is purely coincidental.

It has been suggested (M. A. Shay, private communication) that maximizing the normal-

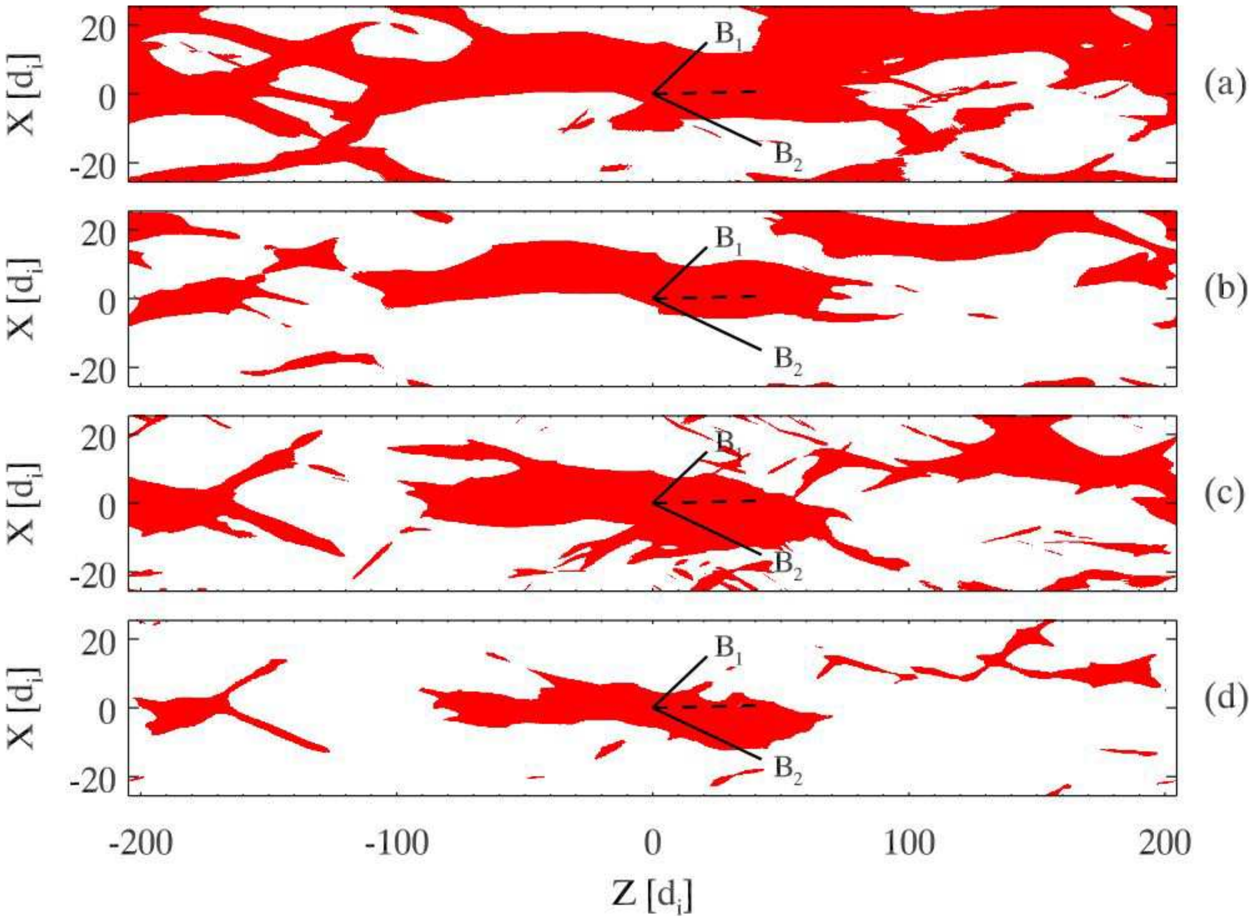

FIG. 4. (Color online) Top view of the isosurfaces of J_{xz} in the upper current layer at $t = 84$ (panels (a) and (b)) and $t = 201$ (panels (c) and (d)). Panels (a) and (c) are at an isosurface level of 1.3, panels (b) and (d) at 1.7. The axes have been shifted to put the prominent features near the center. Solid lines denote the asymptotic magnetic fields and the dashed line the expected orientation of the X-line according to Swisdak and Drake [8]. Note the different axis scales.

ized reconnection rate, and not the outflow speed from the X-line, determines the orientation. If the aspect ratio of the diffusion region (R, assumed to be ≤ 1) remains independent of the upstream properties of the plasma (which has not been established in 3-D simulations) Cassak and Shay [9] argue that the normalized rate E varies as

$$E \sim 2R\,\frac{v_{\rm out}}{c}\left(\frac{B_{1x}B_{2x}}{B_{1x}+B_{2x}}\right). \tag{7}$$

In Fig. 6 the solid and dashed lines trace the dependence of $v_{\rm out}$ and E on α for the parameters of our simulations; the vertical red line gives $\alpha_{\rm sim}$. The dashed line peaks at an angle $\alpha_E = 31.7°$, which is less than α_{SD} and slightly farther away from the value measured in the

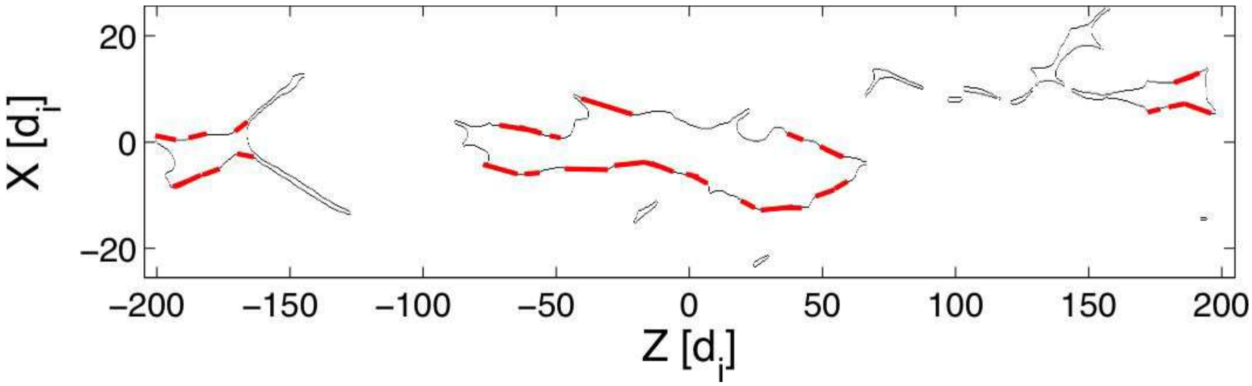

FIG. 5. (Color online) Edges of the projection of the strong current density at $t = 201$ on the $x - z$ plane and detected by the Canny method are shown in black. The red lines are the result of the Hough transform.

simulation. However, given the relatively broad peaks generated by both criteria and the uncertainties associated with determining $\alpha_{\rm sim}$, we cannot reliably discriminate between the two. The similarities between the quantities being maximized means that doing so probably requires extreme choices of parameters (e.g., $B_2/B_1 \gg 1$) that are difficult to simulate.

As can be seen in Fig. 4, the lengths of the X-lines barely change between $t = 84$ and $t = 201$; in fact most growth occurs early in the simulation, before significant magnetic flux has reconnected. We find that the growth of a given X-line is usually throttled by the interaction of its current with islands of reconnected flux from other X-lines at different rational surfaces. This effect will not be present in anti-parallel reconnection (where all of the X-lines are confined to a single plane) and may explain why our result conflicts with the finding of Huba and Rudakov[10] that X-lines continually grow in the current direction. Shay *et al.*[11] did see stagnation of the X-line length for some initial current sheet widths, although not for the value used in this work ($w_0 = 0.5$).

Our results suggest that reconnection can occur in any system where the adjoining fields are not parallel and in which other processes do not suppress reconnection (e.g., diamagnetic drifts[18]). The relatively broad peak of $v_{\rm out}$ in Fig. 6 may mean that, for a given set of asymptotic conditions, X-lines do not take on a single orientation but instead exhibit a distribution of orientations. Further 3-D simulations are needed to test this hypothesis.

We are not aware of any other model that does a better job of predicting α. We suggest that on an encounter with reconnection events in which highly asymmetric conditions exist,

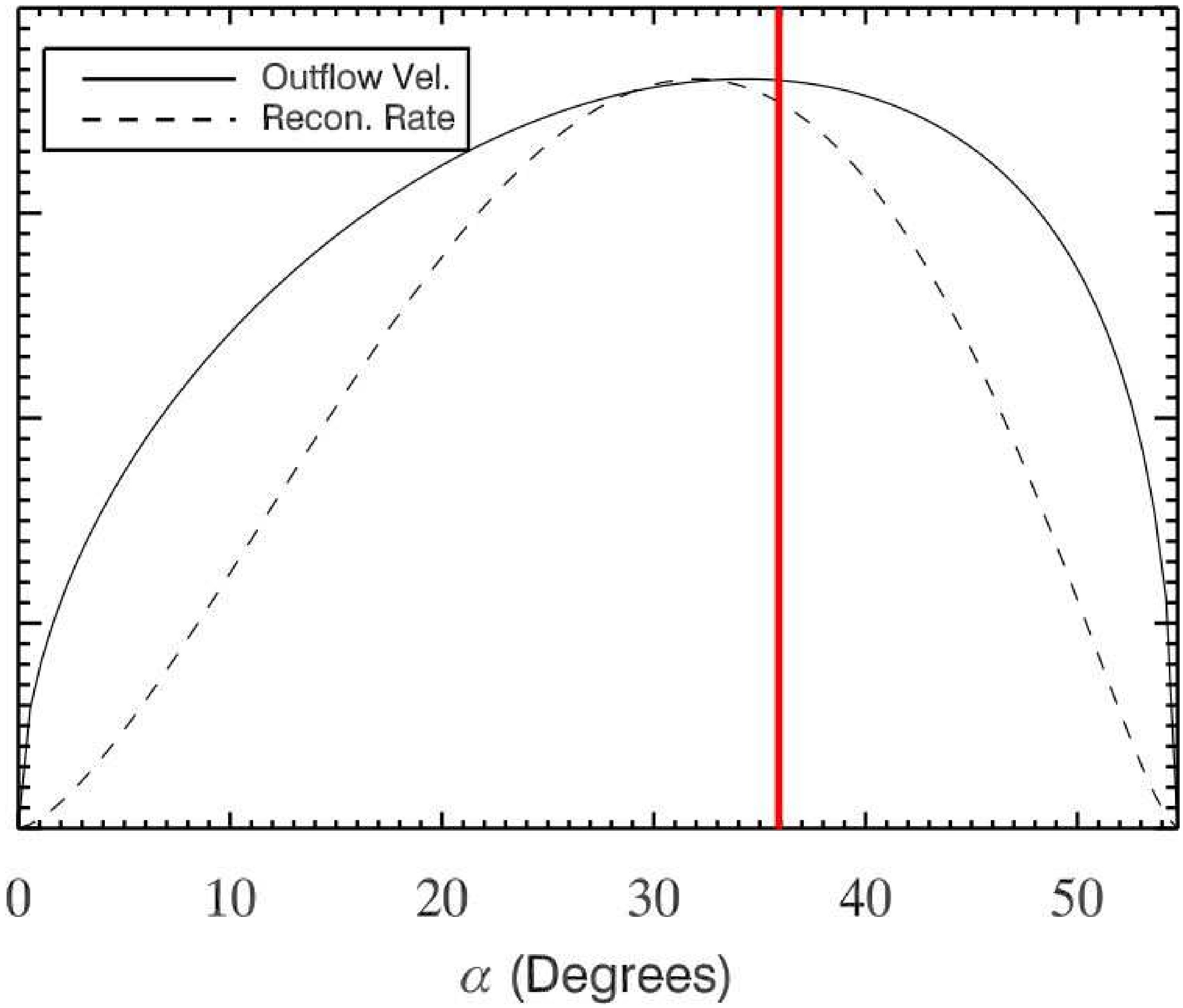

FIG. 6. (Color online) The magnitude of v_{out} (Equation 1) and the normalized reconnection rate of Cassak and Shay[9] (see Equation 7) versus α. The ordinal units are arbitrary and have been suppressed. The vertical red line shows α_{sim} from our three-dimensional simulation.

or while numerically reconstructing such an event, the Swisdak and Drake[8] criterion can cautiously be applied to determine the orientation of the reconnection X-line, as has already been done by Phan, Gosling, and Davis[6] and Teh and Sonnerup[3].

ACKNOWLEDGMENTS

R. S. would like to thank the members of the IREAP group at the University of Maryland for their warm hospitality during his sabbatical year.

REFERENCES

[1]B. U. Ö. Sonnerup, J. Geophys. Res. **79**, 1546 (1974).

[2]S. W. H. Cowley, J. Geophys. Res. **81**, 3455 (1976).

[3]W.-L. Teh and B. U. Ö. Sonnerup, Ann. Geophys. **26**, 2673 (2008).

[4]J. T. Gosling, Ap. J. Lett. **671**, L73 (2007).

[5]J. T. Gosling, T. D. Phan, R. P. Lin, and A. Szabo, Geophys. Res. Lett. **34**, L15110 (2007), 10.1029/2007GL030706.

[6]T. D. Phan, J. T. Gosling, and M. S. Davis, Geophys. Res. Lett. **36**, L09108 (2009), 10.1029/2009GL037713.

[7]T. D. Phan, J. T. Gosling, G. Paschmann, C. Pasma, J. F. Drake, M. Øieroset, D. Larson, R. P. Lin, and M. S. Davis, Astrophys. J.. Lett. **719**, L199 (2010).

[8]M. Swisdak and J. F. Drake, Geophys. Res. Lett. **34**, L11106 (2007), 10.1029/2007GL029815.

[9]P. A. Cassak and M. A. Shay, Phys. Plasmas **14**, 102114 (2007), 10.1063/1.2795630.

[10]J. D. Huba and L. I. Rudakov, Phys. Plasmas **9**, 4435 (2002).

[11]M. A. Shay, J. F. Drake, M. Swisdak, W. Dorland, and B. N. Rogers, Geophys. Res. Lett. **30** (2003), 10.1029/2002GL016267.

[12]G. Lapenta, D. Krauss-Varban, H. Karimabadi, and J. D. Huba, Geophys. Res. Lett. **33**, L10102 (2006), 10.1029/2005GL025124.

[13]M. A. Shay, J. F. Drake, M. Swisdak, and B. N. Rogers, Phys. Plasmas **11**, 2199 (2004).

[14]P. N. Guzdar, J. F. Drake, D. McCrathy, A. B. Hassam, and C. S. Liu, Phys. Fluids B **5**, 3712 (1993).

[15]E. R. Priest, G. Hornig, and D. I. Pontin, J. Geophys. Res. **108**, 1285 (2003).

[16]J. A. Canny, IEEE Trans., Pattern Analysis and Machine Intelligence **8**, 679 (1986).

[17]D. H. Ballard, Pattern Recognition **13**, 111 (1981).

[18]M. Swisdak, B. N. Rogers, J. F. Drake, and M. A. Shay, J. Geophys. Res. **108**, 1218 (2003).